ADVANCED THERAPEUTICS
www.advtherap.com

Mn_3O_4 Nanozyme for Inflammatory Bowel Disease Therapy

*Yuan Cheng, Chaoqun Cheng, Jia Yao, Yijun Yu, Yufeng Liu, He Zhang, Leiying Miao, and Hui Wei**

Recently, reactive oxygen species (ROS) scavenging nanozymes have been developed as natural enzyme alternatives to treat inflammatory bowel disease (IBD) as well as other inflammatory diseases. Among them, manganese oxide nanozymes are advantageous because of remarkable biocompatibility and their good biodegradability. It is herein reported that phospholipid coated Mn_3O_4 nanozymes mimic both superoxide dismutase (SOD) and catalase (CAT) to effectively eliminate ROS that exacerbate inflammation and cause damages to tissues and organs. With the help of phospholipid decoration, the Mn_3O_4 nanozymes are well dispersed and show good stability. Moreover, the coating enables the successful fluorescence labelling to study their biodistribution and fate. Excitingly, the Mn_3O_4 nanozymes exhibit superior therapeutic efficacy for both ulcerative colitis (UC) and Crohn's disease (CD) in mouse models over aminosalicylic acid, a first-line medication for IBD, under the same dosage. Thus, the Mn_3O_4 nanozymes in this work offer a promising nano-medication for inflammation-related disease therapy and broaden the spectrum of biomedical application of nanozymes.

1. Introduction

Inflammatory bowel disease (IBD) is a chronic and refractory immune-mediated disorder. It is estimated that IBD affects over 6.8 million people globally in 2017.[1,2] Ulcerative colitis (UC) and Crohn's disease (CD) are two major forms of IBD that share the common features of abdominal pain, diarrhea, and rectal bleeding. They are often complicated with extra-intestinal manifestation including psoriasis and spondylitis.[3] IBD is drawing much attention not only for its climbing incidence and prevalence, but also for its implication in cancer that causes fatality.[4] The state-of-the-art IBD treatments mainly focus on the remission of inflammation. These treatments, however, suffer from drawbacks in clinical practice, such as insufficient efficacy and side-effects.[5] Therefore, it is of great importance and demand to develop efficient therapeutic methods and discover new strategies for IBD treatment.

Accumulating evidences indicate that reactive oxygen species (ROS) plays a central role in the progress of inflammation including IBD, and its normal level is precisely governed in a homeostatic status in living organisms.[6] To overcome the oxidative stress involved by over-produced ROS, anti-oxidant enzymes such as superoxide dismutase (SOD) and catalase (CAT) were evolved to remove superoxide anion ($^{\bullet}O_2^-$) and hydrogen peroxide (H_2O_2), respectively.[7] Nonetheless, ROS is often overexpressed in the inflamed area of IBD and other inflammatory diseases, and usually could not be sufficiently eliminated by endogenous enzymes to relieve the inflammation.[8] Hence, exogenous ROS scavenging enzymes have been explored for the treatment of IBD.[9] Nevertheless, natural enzymes have several limitations such as high cost, low stability, and potential immunogenicity, which have hindered the use of enzymes in medical applications.[10]

To tackle these challenges, enzyme-like ROS scavenging nanomaterials (termed as nanozymes[11–17]) have been developed to treat IBD as well as other inflammatory diseases.[18–22] For example, ceria nanozyme was engineered to prevent retinal degeneration induced by intracellular peroxides.[23] Nanoceria decorated montmorillonite was developed for IBD therapy.[24] Prussian blue nanozyme was developed to treat liver inflammation and IBD in mouse models.[21,25] Compared with these anti-ROS nanozymes, manganese (Mn)-based nanozymes are very attractive because Mn is one of the most necessary element in

Dr. Y. Cheng, C. Cheng, J. Yao, Dr. Y. Liu, Prof. H. Wei
Department of Biomedical Engineering
College of Engineering and Applied Sciences
Nanjing National Laboratory of Microstructures
Jiangsu Key Laboratory of Artificial Functional Materials
Nanjing University
Nanjing, Jiangsu 210023, China
E-mail: weihui@nju.edu.cn
Y. Yu, Prof. L. Miao
Department of Cariology and Endodontics
Nanjing Stomatological Hospital
Medical School of Nanjing University
Nanjing University
Nanjing, Jiangsu 210093, China
H. Zhang
Department of Periodontology
Nanjing Stomatological Hospital
Medical School of Nanjing University
Nanjing University
Nanjing, Jiangsu 210093, China
Prof. H. Wei
State Key Laboratory of Analytical Chemistry for Life Science and State Key Laboratory of Coordination Chemistry
School of Chemistry and Chemical Engineering
Chemistry and Biomedicine Innovation Center (ChemBIC)
Nanjing University
Nanjing, Jiangsu 210023, China

The ORCID identification number(s) for the author(s) of this article can be found under https://doi.org/10.1002/adtp.202100081

DOI: 10.1002/adtp.202100081

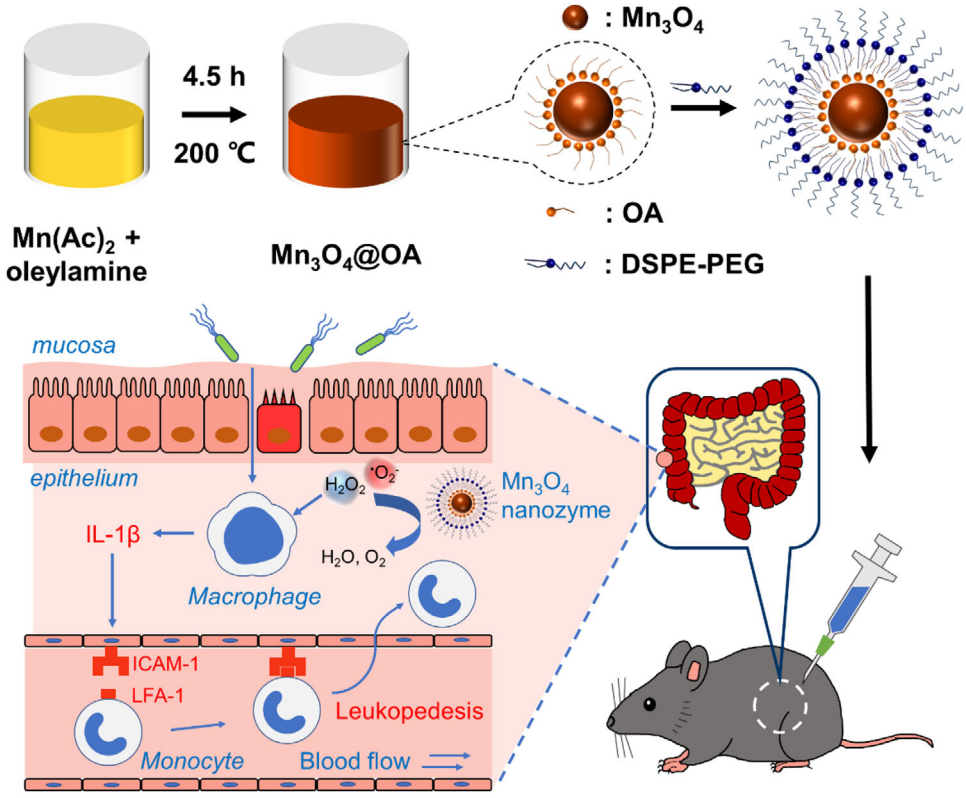

Scheme 1. Schematic illustration of fabrication of Mn_3O_4 nanozyme with ROS scavenging activity for IBD therapy. In the inflamed focus, macrophages sense antigens like microbiomes and generate ROS that stimulate the release of IL-1β. IL-1β upregulates ICAM-1 (intercellular cell adhesion molecule-1, or CD54) on vascular endothelial cells that participate in the pro-inflammatory leukopedesis by interacting with LFA-1 (lymphocyte function-associated antigen-1) expressed on monocytes. The SOD- and CAT-like Mn_3O_4 nanozyme interferes with the transduction cascade of inflammation by scavenging ROS thus ameliorates inflammatory diseases.

organisms and used in Mn-SOD. Mn-based SOD- and CAT-like nanozymes have been demonstrated to possess antioxidation efficacy toward cell protection and therapy for inflammation-related disease.[26–28] Recently, attempts have been made to evaluate the therapeutic efficacy of Mn-porphyrin based nanozyme on IBD mouse model.[22] In our previous work, a hydro-thermally synthesized Mn_3O_4 nanozyme with both SOD- and CAT-like activities was utilized in vivo for an acute inflammation model.[29] The biodegradability of Mn_3O_4 nanoparticles (NPs) avoids the retention in tissues and organs thus minimizes their accumulative and long-term toxicity compared to non-biodegradable Mn-based nanozymes.[30]

To advance the biomedical application of Mn_3O_4 nanozyme, here we demonstrated that Mn_3O_4 NPs synthesized via a solvent-thermal method possessed remarkable both SOD- and CAT-like activities. When the Mn_3O_4 NPs were decorated with phospholipid of 1, 2-distearoyl-sn-glycero-3-phosphoethanolamine-*N*-[carboxy(polyethylene glycol)] (DSPE-PEG), it endowed the Mn_3O_4 NPs excellent dispersibility and biocompatibility in aqueous medium.[31] The Mn_3O_4 NPs were further applied to the therapy of UC and CD models (**Scheme 1**). Our results showed that Mn_3O_4 NPs targeted and scavenged ROS evolved by macrophages thus sequestrated interleukin (IL)-1β (a crucial proinflammatory cytokine). Moreover, they exhibited enhanced therapeutic efficacy than 5-aminosalicylic acid (5-ASA), a first-line medication for both UC and CD therapy, under the same dosage.[5] Due to the superior SOD- and CAT-like activities, the Mn_3O_4 NPs as low as the dosage of 0.1 mg kg^{-1} body weight remarkably ameliorated both UC and CD model mice without apparent acute or long-term toxicity of the Mn_3O_4 NPs. The results in this work not only demonstrated the superior effectiveness of ROS scavenging nanozyme for IBD therapy, but also provided the practical feasibility of biomedical applications of nanozymes.

2. Results and Discussion

Mn_3O_4 was synthesized through the solvent-thermal method by using oleylamine (OA) as capping agents. The synthesized Mn_3O_4@OA NPs were spherical and had a diameter of around 10 nm (**Figure 1**a). The Mn_3O_4@OA NPs were further cladded with DSPE-PEG to obtain hydrophilic Mn_3O_4@OA@DSPE-PEG NPs (termed as Mn_3O_4 NPs for short below) (Figure 1b). The Mn_3O_4 NPs kept uniform morphology with narrowly dispersed size and exhibited characteristic infrared absorption of Mn_3O_4@OA NPs and DSPE-PEG (Figure S1b, Supporting Information), which indicated that the Mn_3O_4 NPs were successfully prepared and suitable for further application of IBD therapy.

The DSPE-PEG coating remarkably enhanced the stability of Mn_3O_4 NPs in phosphate buffered saline (PBS) and glutathione (GSH) compared with naked Mn_3O_4 nanozymes in our

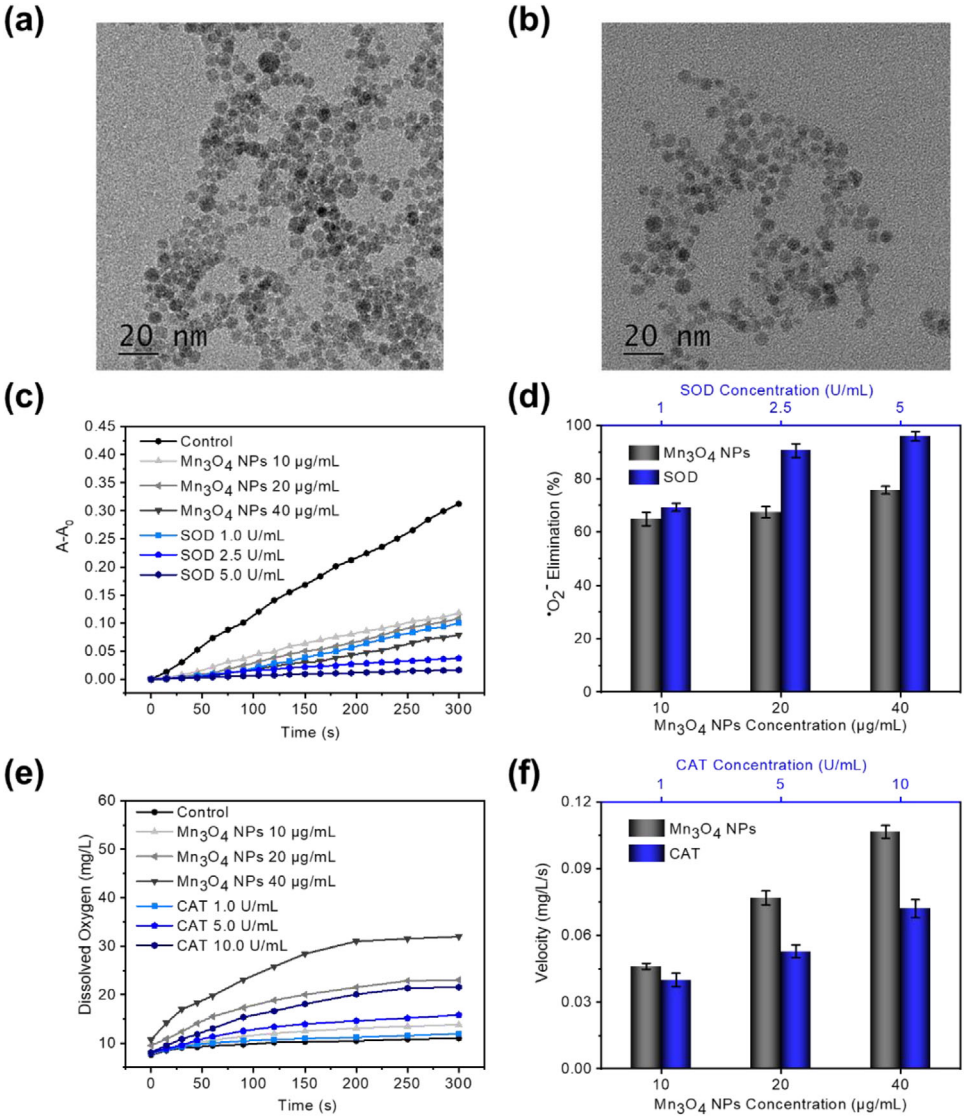

Figure 1. Morphology and ROS scavenging activities of Mn_3O_4 NPs. TEM images of a) Mn_3O_4@OA and b) Mn_3O_4@OA@DSPE-PEG. c) Typical kinetic curves of A-A0 (550 nm) for monitoring the reduction of NBT with xanthine and xanthine oxidase in the absence and presence of Mn_3O_4 nanozyme and SOD. d) Dependence between the $^{\bullet}O_2^-$ elimination efficiency and concentrations Mn_3O_4 NPs and SOD. e) Typical kinetic curves of oxygen generation from the decomposition of H_2O_2 (40 mM) in the absence and presence of Mn_3O_4 NPs and CAT. f) Dependence between the oxygen production velocities in the initial 60 s and concentrations of Mn_3O_4 NPs and CAT.

previous work (Figure S2, Supporting Information) and prevented the burst release of Mn^{2+}, without altering biodegradable nature of Mn_3O_4 NPs.[29] Moreover, the terminal carboxyl group of DSPE-PEG gifted the Mn_3O_4 NPs with feasibility of functionalization such as fluorescence labelling (Figure 5a). By utilizing the quantitative method in Figure S2, Supporting Information, the element content of Mn was determined as 0.181 ± 0.015 mg in 1.000 mg of the Mn_3O_4 NPs, and the dosage in the following in vitro and in vivo experiments was calculated by the Mn_3O_4@OA@DSPE-PEG NPs that contained pure Mn_3O_4 ≈25 wt% of the total weight.

The in vitro ROS scavenging capacity of the Mn_3O_4 NPs was firstly investigated by SOD- and CAT-like activities assay of transforming $^{\bullet}O_2^-$ and H_2O_2, respectively. The SOD-like activity of the Mn_3O_4 NPs was carried out by monitoring absorbance of nitrotetrazolium blue chloride (NBT) at 550 nm, which can specifically be reduced by $^{\bullet}O_2^-$ generated from the mixture of xanthine and xanthine oxidase. The $^{\bullet}O_2^-$ scavenging activities of both Mn_3O_4 NPs and SOD exhibited dose-dependent manner (Figure 1c). The activity of 10 μg mL^{-1} of Mn_3O_4 NPs was close to that of 1 U mL^{-1} of SOD (Figure 1d), which was calculated with the absorption value compared with control at the end of the experiments (300 s). The CAT-like activity of the Mn_3O_4 NPs was further verified by determination of O_2 from H_2O_2 decomposition, and similar results were observed (Figure 1e,f). The results above demonstrated that the Mn_3O_4 NPs possessed both SOD- and CAT-like activities and were comparable to 1 U mL^{-1} of both SOD and CAT at the concentration of 10 μg mL^{-1}.

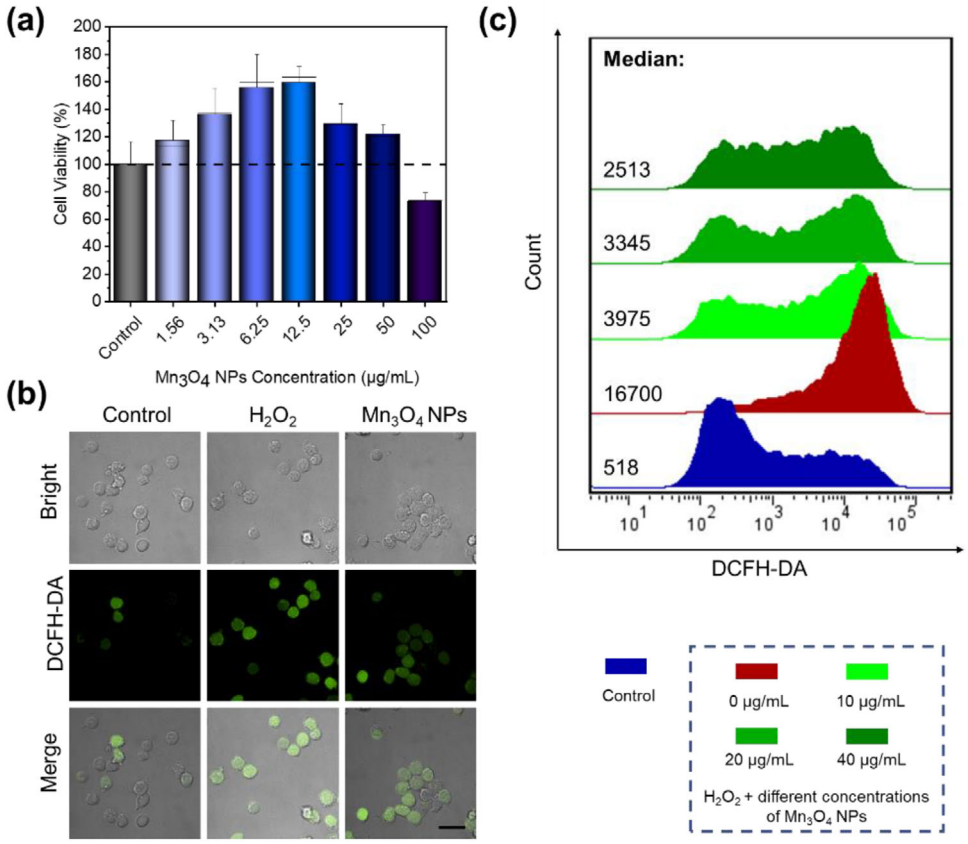

Figure 2. Cytotoxicity and ROS scavenging activities of Mn_3O_4 NPs in cultured cells. a) Cytotoxicity of Mn_3O_4 NPs in cultured RAW 264.7 cells determined by CCK-8 assay. ROS scavenging activities of Mn_3O_4 NPs in 100 μM H_2O_2 stimulated RAW 264.7 cells investigated by b) confocal scanning laser microscopy and c) determined with flow cytometry. Scale bar = 25 μm.

It is of importance to investigate the biocompatibility of the nanomaterials before their biomedical application. Therefore, the cytotoxicity of the Mn_3O_4 NPs toward murine macrophages (RAW 264.7) was investigated by CCK (Cell Counting Kit)-8 assay. The result indicated that the Mn_3O_4 NPs exhibited no cytotoxicity toward RAW 264.7 cells within 50 μg mL^{-1} (**Figure 2**a). The in vitro ROS scavenging capacity of the Mn_3O_4 NPs in co-cultured 100 μM H_2O_2 stimulated RAW 264.7 cells was preliminarily visualized by confocal scanning laser microscopy imaging (Figure 2b). It showed that the Mn_3O_4 NPs partially decreased the fluorescence intensity that evolved by 2,7-dichlorodihydrofluorescein diacetate (DCFH-DA, a fluorescence dye for intracellular ROS) in H_2O_2 treated RAW 264.7 cells. The intracellular ROS was further quantitatively analyzed by flow cytometry, and the median of the fluorescence intensity (Figure 2c) demonstrated that the Mn_3O_4 NPs exhibited dose-dependent ROS scavenging capacity and significantly relieved oxidative stress of RAW 264.7 cells. The results above indicated that the Mn_3O_4 NPs exhibited satisfactory cellular protective efficacy and excellent intracellular ROS scavenging capacity at the concentration of 10 μg mL^{-1}.

On the basis of the excellent ROS scavenging activity and satisfactory biocompatibility of Mn_3O_4 NPs, the in vivo therapeutic efficacy of Mn_3O_4 NPs was then investigated for the treatment of UC and CD in murine models of the disease states. Dextran sulfate sodium (DSS)-induced UC model was preliminarily established to verify the effectiveness of Mn_3O_4 NPs, and the over-all procedure is shown as **Figure 3**a.[32] The body weights of DSS-induced groups exhibited remarkable decrease after 6 consecutive days (Figure 3b), which indicated the successful onset of UC together with shortened colon lengths induced by DSS (Figure 3c) and inflammatory infiltration (Figure 3d). After that, different dosages of Mn_3O_4 NPs were intraperitoneally injected to each mouse on three consecutive days (days 7, 8, and 9), and the treatments relieved body weight loss and colon length shortening on day 10 at different levels. To our surprise, the Mn_3O_4 NPs as low as 0.1 mg kg^{-1} exhibited the best efficacy among the dosages in this experiment, and increasing dosage did not result in better efficacy, which could be explained that the high performance of ROS scavenging Mn_3O_4 NPs already effectively mitigated the UC at the dose of 0.1 mg kg^{-1}, and over-dosing was not beneficial but burdened the metabolism of Mn_3O_4 NPs.

To further elucidate the therapeutic efficacy of Mn_3O_4 NPs, DSS-induced UC model was established again to evaluate Mn_3O_4 NPs together with 5-ASA, a first-line medication for IBD treatment, as a positive control.[5] As shown in **Figure 4**a,b, 0.1 mg kg^{-1} of Mn_3O_4 NPs still exhibited remarkable therapeutic efficacy while 5-ASA did not at the same dosage. Meanwhile, decreasing the dosage of Mn_3O_4 NPs to 0.01 mg kg^{-1} did not embrace apparent anti-inflammation effect, indicating that 0.1 mg kg^{-1} of

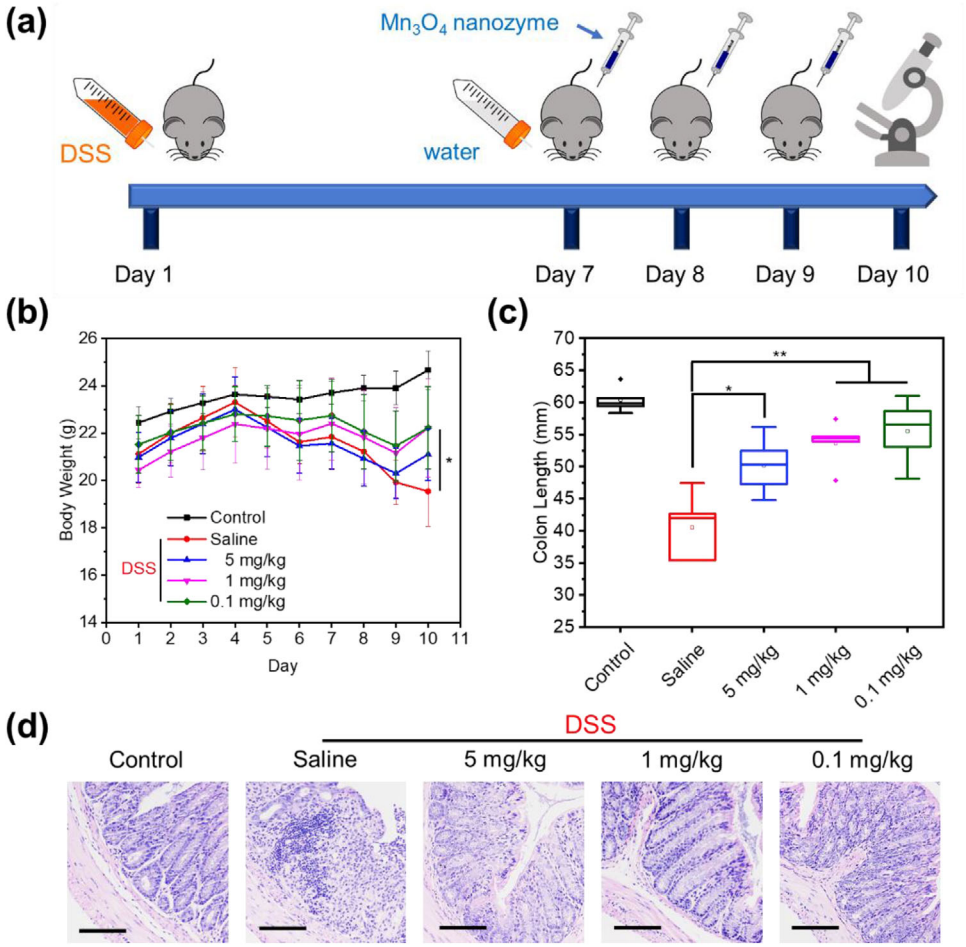

Figure 3. UC therapy with Mn_3O_4 NPs. a) Overall procedure of the animal experiment (DSS-induced colitis). b) Daily body-weight development for 10 days. c) The corresponding colon lengths in indicated groups. d) H&E-stained colonic sections of mice from indicated groups on day 10, scale bar = 100 μm. The data are shown as mean ± SD ($n = 5$). *$p < 0.05$, **$p < 0.01$; t test.

Mn_3O_4 NPs was the optimized dosage according to the experiments above. To verify the therapeutic effect was evolved by the ROS scavenging Mn_3O_4 NPs not the decomposed Mn_3O_4 such as Mn^{2+} or component DSPE-PEG, the Mn_3O_4 NPs was resolved by stoichiometric HCl (Figure S1e, Supporting Information) and re-dispersed in PBS at the same Mn concentration with 0.1 mg kg^{-1} of treated Mn_3O_4 NPs, and designated as Mn^{2+} for short. According to the results in Figure 4a,b,e, Mn^{2+} did not exhibit obvious anti-inflammation effect, which demonstrated that the therapeutic effect of UC was from ROS scavenging Mn_3O_4 NPs rather than Mn^{2+} or any degraded components.

The remission capacity of Mn_3O_4 NPs in the focus of UC was investigated with the determination of pro-inflammatory cytokines by enzyme linked immunosorbent assay (ELISA). As shown in Figure 4c,d, the levels of tumor necrosis factor-α (TNF-α) and IL-1β were both significantly elevated in colon tissues of UC model, and effectively sequestrated by 0.1 mg kg^{-1} of Mn_3O_4 NPs treatment. The possible mechanism of anti-inflammation efficacy of Mn_3O_4 NPs is summarized in Figure 4f. In the process of colitis, epithelia activate the NADPH oxidase (NOX) to generate $^{\bullet}O_2^-$ and H_2O_2 in response to pathogen-associated molecular patterns (PAMPs) and danger-associated molecular patterns (DAMPs), and the ROS could trigger NOD-, LRR- and pyrin domain-containing 3 (NLRP3) inflammasome that lead to IL-1β and IL-18 production, which stimulates the accumulation of T helper (T_H) 17 cells.[33] On the other hand, IL-1β can induce macrophages to generate downstream IL-6, which together evoke the activation of T_H1 or T_H2 cells that propagate CD and UC, respectively, while T_H17 cells is responsible for both CD and UC.[34,35] Now that ROS is one of important trigger for IL-1β and IL-18 production and lymphatic infiltration, which aggravate the severity of IBD, ROS scavenging Mn_3O_4 NPs may be an effective therapeutic agent for the treatment that target and eliminate the ROS in upstream of inflammation signaling.

The in vivo behavior of treated Mn_3O_4 NPs is crucial for its therapy validation and further application, and fluorescence labelling of Mn_3O_4 NPs was executed by covalent conjugation of aminofluorescein with carboxyl terminated DSPE-PEG capped Mn_3O_4 NPs (**Figure 5**a). The obtained fluorescein labeled Mn_3O_4 NPs (Figure S1f, Supporting Information) can be visualized with in vivo fluorescence imaging (Figure 5b) without obviously changing the particle size or zeta potential (Figure S1i,j, Supporting Information). The biodistribution of fluorescein labeled Mn_3O_4 NPs is shown in Figure 5c. It can be seen that Mn_3O_4

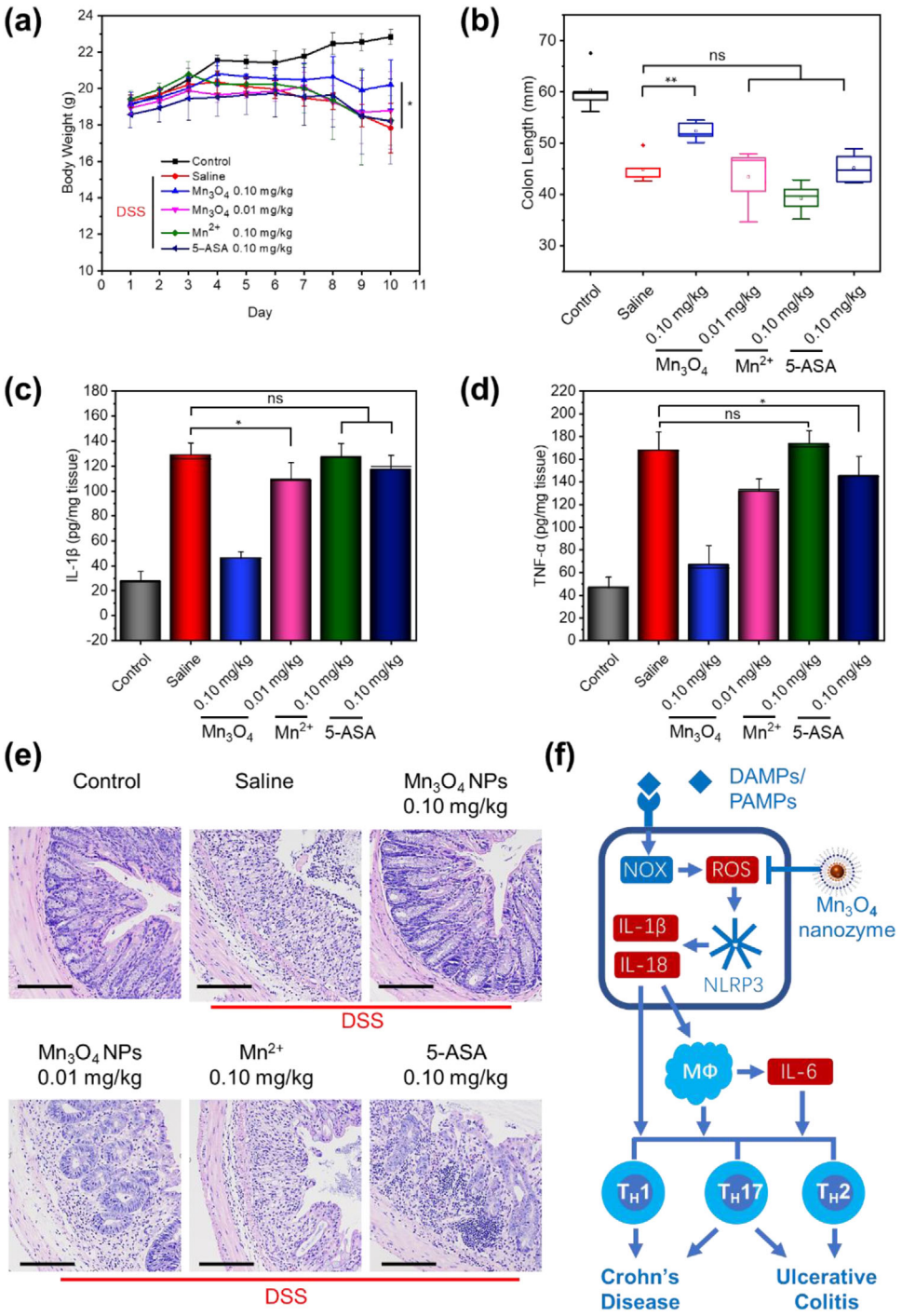

Figure 4. UC therapy with Mn_3O_4 NPs compared with 5-ASA. a) Daily body-weight development for 10 days. b) The corresponding colon lengths in indicated groups. c) IL-1β and d) TNF-α levels in colon homogenates from indicated groups. e) H&E stained colonic sections of mice from indicated groups on day 10, scale bar = 100 µm. f) Possible mechanism of anti-inflammation efficacy of Mn_3O_4 NPs. The data are shown as mean ± SD ($n = 5$). *$p < 0.05$, **$p < 0.01$; ns = not significant; t test.

NPs mainly accumulated in liver 4 h after intraperitoneal injection and were gradually excreted into colon, which reaching its intensity peak after 24 h. Since liver is primary organ that process the Mn_3O_4 NPs, the metabolism of which and redox status of liver was necessarily investigated by GSH and oxidized GSH (GSSG) assay. From Figure S4b, Supporting Information, it can be observed that Mn_3O_4 NPs did not decrease the GSH level 6 h after intraperitoneal injection, while decomposed Mn^{2+} remarkably depleted the GSH in a dose-dependent manner. Together with Figure S4e, Supporting Information, the GSH/GSSG ratio

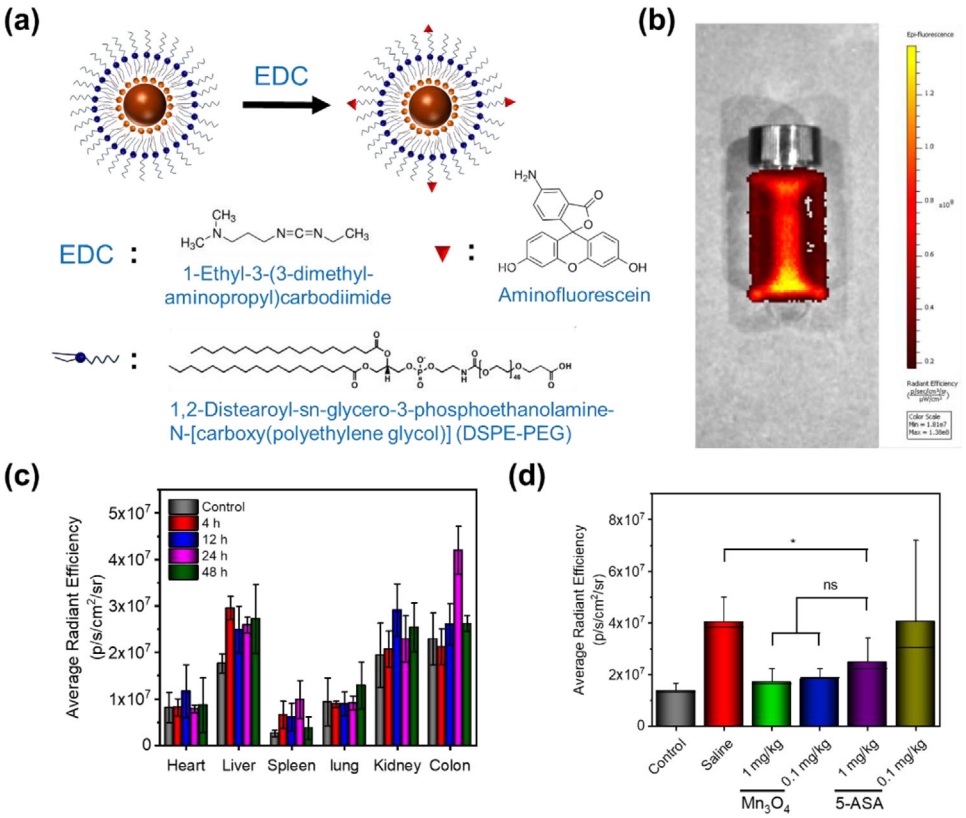

Figure 5. ROS scavenging efficiency and biodistribution of Mn_3O_4 NPs in mice. a) Conjugation of aminofluorescein with carboxyl terminated DSPE-PEG decorated Mn_3O_4 NPs. b) Fluorescence image of fluorescein labeled Mn_3O_4 NPs (25 μg mL^{-1}). c) Ex vivo biodistribution of fluorescein labeled Mn_3O_4 NPs in treated mice. The data are shown as mean ± SD ($n = 3$). d) Ex vivo fluorescence intensity of colons from indicated groups 0.5 h after intraperitoneal injection of 0.7 mg DCFH-DA per mouse. The data are shown as mean ± SD ($n = 4$). *$p < 0.05$; ns = not significant; t test.

manifested that Mn_3O_4 NPs exhibited negligible harmful effects on the liver within 6 h of treatment, but Mn^{2+} exerted obvious decrease of both GSH level and GSH/GSSG ratio. As shown in Figure S4d,e, Supporting Information, 0.1 mg kg^{-1} of Mn_3O_4 NPs was much safer than that of 5.0 mg kg^{-1} toward GSH and GSH/GSSG ratio in the liver, indicated that the dosage of 0.1 mg kg^{-1} was appropriate for in vivo treatment. It also can be seen that no obvious histopathological change in major organs of mice 7 days or 30 days receiving intraperitoneal injection Mn_3O_4 NPs at the dose of 1.0 mg kg^{-1} (Figure S4a, Supporting Information), which further guaranteed the biosafety of Mn_3O_4 NPs.

As mentioned above, ROS scavenging Mn_3O_4 NPs may be pharmacologically effective for both UC and CD, thus it is of importance to verify the therapeutic efficacy of Mn_3O_4 NPs toward CD, another major form of IBD. The 2,4,6-trinitro benzene sulfonic acid (TNBS) induced CD model[32] is established as **Figure 6**a to evaluate Mn_3O_4 NPs compared with 5-ASA. Briefly, on day 1, mice were presensitized by absorption of TNBS solution through the preserved skin on the back (Figure S7b, Supporting Information). 7 days later, on day 8, mice were slowly administered TNBS solution into the colon lumen to induce CD. In addition to an untreated control group, a Sham group was also used in which the TNBS solution was replaced with equal volume of saline. The successful onset of CD was indicated by body weight loss on day 9 for all TNBS-treated groups (Figure 6b). Mn_3O_4 NPs and 5-ASA were administered by intraperitoneal injection to the mice on 3 consecutive days (days 9, 10, and 11), respectively. Comparison of body weight changes and colon lengths recovery demonstrated the considerable therapeutic efficacy of Mn_3O_4 NPs at the concentrations of both 1.0 and 0.1 mg kg^{-1} (Figure 6b,c). By comparison, the group treated with 5-ASA at 1.0 mg kg^{-1} exhibited restricted remissive effect while 0.1 mg kg^{-1} of 5-ASA showed no obvious therapeutic effect on CD, which was in accordance with IL-1β and TNF-α levels and pathological observation (Figure 6d,e,f). Thus, it is demonstrated that Mn_3O_4 NPs directly and effectively alleviate disease by scavenging ROS that have a potentially greater breadth and efficacy compared to traditional small molecular medications in IBD treatment.

3. Conclusion

The monodispersed and biodegradable Mn_3O_4 NPs with in vitro and in vivo ROS scavenging capacity were fabricated and verified in this work. The DSPE-PEG coating not only increased the dispersity and stability of Mn_3O_4 NPs in physiological environment, but also endowed the post-functionality and biocompatibility. The remarkable biosafety and ROS scavenging capacity of Mn_3O_4 NPs was also investigated in vitro and in vivo. For both UC and CD treatments, the therapeutic efficacy of Mn_3O_4 NPs at the dose of 0.1 mg kg^{-1} was verified and superior to 5-ASA at

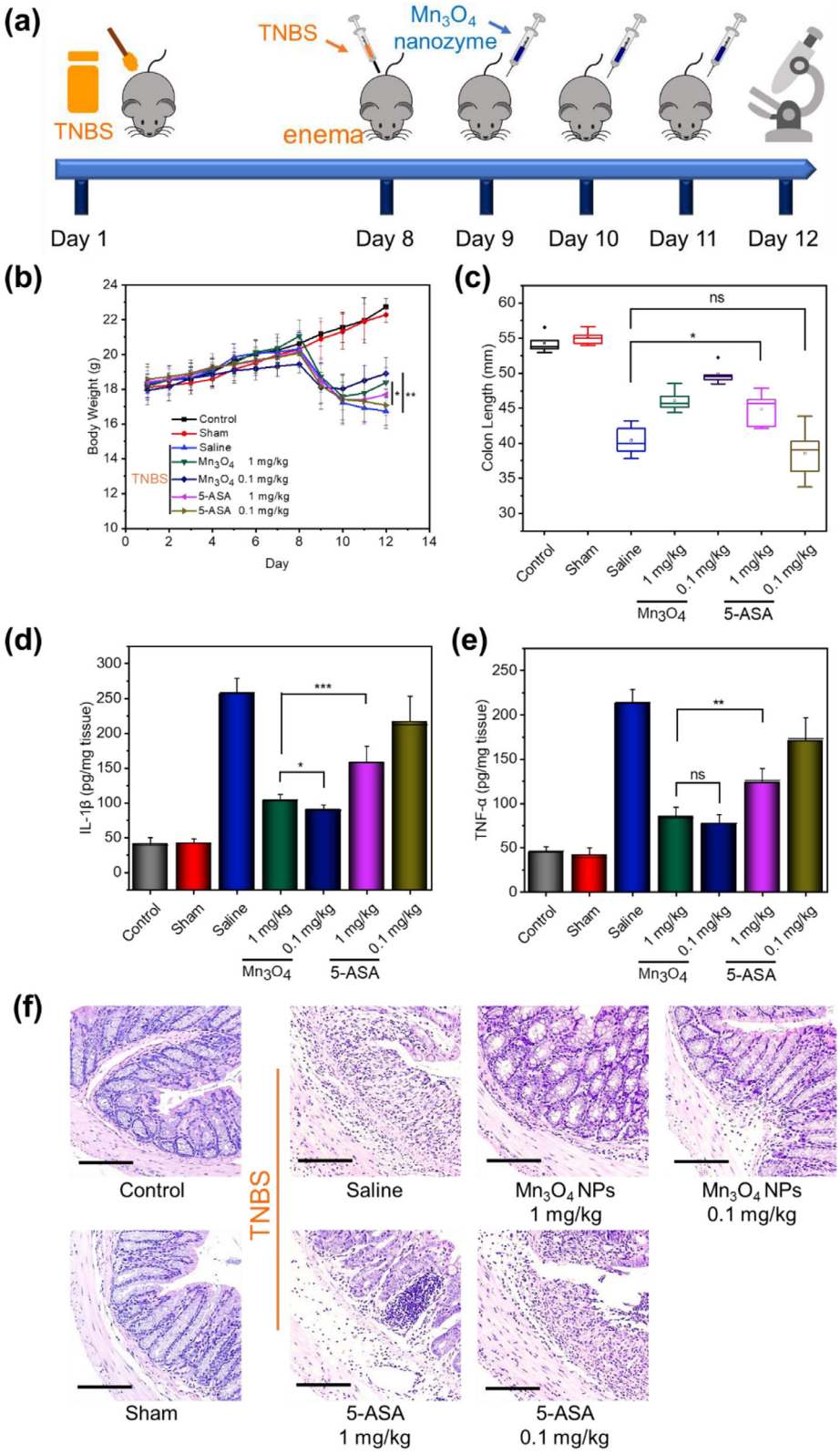

Figure 6. CD therapy with Mn_3O_4 NPs. a) Overall procedure of the animal experiment of TNBS-induced colitis. b) Daily body-weight development for 12 days. c) The corresponding colon lengths in indicated groups. d) IL-1β and e) TNF-α levels in colon homogenates from indicated groups. f) H&E stained colonic sections of mice from indicated groups on day 12, scale bar = 100 μm. The data are shown as mean ± SD ($n = 5$). *$p < 0.05$, **$p < 0.01$, ***$p < 0.005$; ns = not significant; t test.

the same dosage. The Mn_3O_4 NPs in this work revealed effective IBD therapeutic efficacy by targeting ROS, and broadened the spectrum of biomedical application of nanozymes.

4. Experimental Section

All the animal studies were approved by the Committee for Experimental Animals Welfare and Ethics of Nanjing Drum Tower Hospital, the Affiliated Hospital of Nanjing University Medical School (Approval number 20181204). Further details on procedures and instrumentation are given in the Supporting Information.

Supporting Information

Supporting Information is available from the Wiley Online Library or from the author.

Acknowledgements

Y.C. and C.C. contributed equally to this work. This work was supported by the National Key R&D Program of China (2019YFA0709200), the National Natural Science Foundation of China (21874067 and 21722503), the Natural Science Foundation of Jiangsu Province (BK20180340), CAS Interdisciplinary Innovation Team (JCTD-2020-08), PAPD Program, and Fundamental Research Funds for the Central Universities (021314380145, 021414380485, and YK2005002).

Conflict of Interest

The authors declare no conflict of interest.

Data Availability Statement

Research data are not shared.

Keywords

anti-inflammation, inflammatory bowel disease, Mn_3O_4, nanozyme, reactive oxygen species

Received: March 31, 2021
Revised: May 9, 2021
Published online: June 19, 2021

[1] G. G. Kaplan, *Nat. Rev. Gastroenterol. Hepatol.* **2015**, *12*, 720.
[2] S. Alatab, S. G. Sepanlou, K. Ikuta, H. Vahedi, C. Bisignano, S. Safiri, A. Sadeghi, M. R. Nixon, A. Abdoli, H. Abolhassani, V. Alipour, M. A. H. Almadi, A. Almasi-Hashiani, A. Anushiravani, J. Arabloo, S. Atique, A. Awasthi, A. Badawi, A. A. A. Baig, N. Bhala, A. Bijani, A. Biondi, A. M. Borzi, K. E. Burke, F. Carvalho, A. Daryani, M. Dubey, A. Eftekhari, E. Fernandes, J. C. Fernandes, et al., *The Lancet Gastroenterol. Hepatol.* **2020**, *5*, 17.
[3] J. H. Cho, *Nat. Rev. Immunol.* **2008**, *8*, 458.
[4] L. Beaugerie, S. H. Itzkowitz, *N. Engl. J. Med.* **2015**, *372*, 1441.
[5] B. Bressler, J. K. Marshall, C. N. Bernstein, A. Bitton, J. Jones, G. I. Leontiadis, R. Panaccione, A. H. Steinhart, F. Tse, B. Feagan, Toronto Ulcerative Colitis Consensus Group, *Gastroenterology* **2015**, *148*, 1035.e1033.
[6] K. J. Maloy, F. Powrie, *Nature* **2011**, *474*, 298.
[7] J. M. MatÉs, C. Pérez-Gómez, I. N. De Castro, *Clin. Biochem.* **1999**, *32*, 595.
[8] J. R. Korzenik, D. K. Podolsky, *Nat. Rev. Drug Discovery* **2006**, *5*, 197.
[9] T. T. Jubeh, M. Nadler-Milbauer, Y. Barenholz, A. Rubinstein, *J. Drug Targeting* **2006**, *14*, 155.
[10] H. Wei, E. Wang, *Chem. Soc. Rev.* **2013**, *42*, 6060.
[11] L. Huang, J. Chen, L. Gan, J. Wang, S. Dong, *Sci. Adv.* **2019**, *5*, eaav5490.
[12] M. S. Kim, S. Cho, S. H. Joo, J. Lee, S. K. Kwak, M. I. Kim, J. Lee, *ACS Nano* **2019**, *13*, 4312.
[13] C. Wang, F. Cao, Y. Ruan, X. Jia, W. Zhen, X. Jiang, *Angew. Chem., Int. Ed.* **2019**, *58*, 9846.
[14] X. Hu, F. Li, F. Xia, X. Guo, N. Wang, L. Liang, B. Yang, K. Fan, X. Yan, D. Ling, *J. Am. Chem. Soc.* **2020**, *142*, 1636.
[15] X. Zhang, Y. Liu, S. Gopalakrishnan, L. Castellanos-Garcia, G. Li, M. Malassiné, I. Uddin, R. Huang, D. C. Luther, R. W. Vachet, V. M. Rotello, *ACS Nano* **2020**, *14*, 4767.
[16] K. Fan, J. Xi, L. Fan, P. Wang, C. Zhu, Y. Tang, X. Xu, M. Liang, B. Jiang, X. Yan, L. Gao, *Nat. Commun.* **2018**, *9*, 1440.
[17] S. Maiti, I. Fortunati, C. Ferrante, P. Scrimin, L. J. Prins, *Nat. Chem.* **2016**, *8*, 725.
[18] Z. Zhang, X. Zhang, B. Liu, J. Liu, *J. Am. Chem. Soc.* **2017**, *139*, 5412.
[19] W. Zhen, Y. Liu, L. Lin, J. Bai, X. Jia, H. Tian, X. Jiang, *Angew. Chem., Int. Ed.* **2018**, *57*, 10309.
[20] J. Wu, X. Wang, Q. Wang, Z. Lou, S. Li, Y. Zhu, L. Qin, H. Wei, *Chem. Soc. Rev.* **2019**, *48*, 1004.
[21] J. Zhao, W. Gao, X. Cai, J. Xu, D. Zou, Z. Li, B. Hu, Y. Zheng, *Theranostics* **2019**, *9*, 2843.
[22] Y. Liu, Y. Cheng, H. Zhang, M. Zhou, Y. Yu, S. Lin, B. Jiang, X. Zhao, L. Miao, C.-W. Wei, Q. Liu, Y.-W. Lin, Y. Du, C. J. Butch, H. Wei, *Sci. Adv.* **2020**, *6*, eabb2695.
[23] J. Chen, S. Patil, S. Seal, J. F. McGinnis, *Nat. Nanotechnol.* **2006**, *1*, 142.
[24] S. Zhao, Y. Li, Q. Liu, S. Li, Y. Cheng, C. Cheng, Z. Sun, Y. Du, C. J. Butch, H. Wei, *Adv. Funct. Mater.* **2020**, *30*, 2004692.
[25] W. Zhang, S. Hu, J.-J. Yin, W. He, W. Lu, M. Ma, N. Gu, Y. Zhang, *J. Am. Chem. Soc.* **2016**, *138*, 5860.
[26] Y. Ning, Y. Huo, H. Xue, Y. Du, Y. Yao, A. C. Sedgwick, H. Lin, C. Li, S.-D. Jiang, B.-W. Wang, S. Gao, L. Kang, J. L. Sessler, J.-L. Zhang, *J. Am. Chem. Soc.* **2020**, *142*, 10219.
[27] R. Ragg, A. M. Schilmann, K. Korschelt, C. Wieseotte, M. Kluenker, M. Viel, L. Völker, S. Preiß, J. Herzberger, H. Frey, K. Heinze, P. Blümler, M. N. Tahir, F. Natalio, W. Tremel, *J. Mater. Chem. B* **2016**, *4*, 7423.
[28] N. Singh, M. A. Savanur, S. Srivastava, P. D'Silva, G. Mugesh, *Angew. Chem., Int. Ed.* **2017**, *56*, 14267.
[29] J. Yao, Y. Cheng, M. Zhou, S. Zhao, S. Lin, X. Wang, J. Wu, S. Li, H. Wei, *Chem. Sci.* **2018**, *9*, 2927.
[30] B. Wang, X. He, Z. Zhang, Y. Zhao, W. Feng, *Acc. Chem. Res.* **2013**, *46*, 761.
[31] J. Li, Y. Yang, L. Huang, *J. Controlled Release* **2012**, *158*, 108.
[32] S. Wirtz, V. Popp, M. Kindermann, K. Gerlach, B. Weigmann, S. Fichtner-Feigl, M. F. Neurath, *Nat. Protoc.* **2017**, *12*, 1295.
[33] E. L. Campbell, S. P. Colgan, *Nat. Rev. Gastroenterol. Hepatol.* **2019**, *16*, 106.
[34] H. S. P. de Souza, C. Fiocchi, *Nat. Rev. Gastroenterol. Hepatol.* **2016**, *13*, 13.
[35] M. F. Neurath, *Nat. Rev. Immunol.* **2014**, *14*, 329.

